[11] Tokunaga K, Matsuzawa Y, Ishikawa K, et al. A novel technique for the determination of body fat by computed tomography. Int J Obes 1983;7:437–45.
[12] Teramoto T, Sasaki J, Ueshima H, et al. Executive summary of Japan Atherosclerosis Society (JAS) guideline for diagnosis and prevention of atherosclerotic cardiovascular diseases for Japanese. J Atheroscler Thromb 2007;14:45–50.
[13] Matsuzawa Y. Metabolic syndrome-definition and diagnostic criteria in Japan. J Atheroscler Thromb 2005;12:301.
[14] Agatston AS, Janowitz WR, Hildner FJ, et al. Quantification of coronary artery calcium using ultrafast computed tomography. J Am Coll Cardiol 1990;15:827–32.
[15] Reilly MP, Wolfe ML, Localio AR, et al. Coronary artery calcification and cardiovascular risk factors: impact of the analytic approach. Atherosclerosis 2004;173:69–78.
[16] Youden WJ. Index for rating diagnostic tests. Cancer 1950;3:32–5.
[17] Arad Y, Newstein D, Cadet F, et al. Association of multiple risk factors and insulin resistance with increased prevalence of asymptomatic coronary artery disease by an electron-beam computed tomographic study. Arterioscler Thromb Vasc Biol 2001;21:2051–8.
[18] Lee CD, Jacobs Jr DR, Schreiner PJ, et al. Abdominal obesity and coronary artery calcification in young adults: the Coronary Artery Risk Development in Young Adults (CARDIA) Study. Am J Clin Nutr 2007;86:48–54.
[19] Elkeles RS, Feher MD, Flather MD, et al. The association of coronary calcium score and conventional cardiovascular risk factors in Type 2 diabetic subjects asymptomatic for coronary heart disease (The PREDICT Study). Diab Med 2004;21:1129–34.
[20] Mazzone T, Meyer PM, Kondos GT, et al. Relationship of traditional and nontraditional cardiovascular risk factors to coronary artery calcium in type 2 diabetes. Diabetes 2007;56:849–55.
[21] Rosito GA, Massaro JM, Hoffmann U, et al. Pericardial fat, visceral abdominal fat, cardiovascular disease risk factors, and vascular calcification in a community-based sample: the Framingham Heart Study. Circulation 2008;117:605–13.
[22] Lind L. Endothelium-dependent vasodilation, insulin resistance and the metabolic syndrome in an elderly cohort: the Prospective Investigation of the Vasculature in Uppsala Seniors (PIVUS) study. Atherosclerosis 2008;196:795–802.
[23] Basili S, Pacini G, Guagnano MT, et al. Insulin resistance as a determinant of platelet activation in obese women. J Am Coll Cardiol 2006;48:2531–8.
[24] Lau DC, Dhillon B, Yan H, et al. Adipokines: molecular links between obesity and atherosclerosis. Am J Physiol Heart Circ Physiol 2005;288:2031–41.
[25] Nishida M, Moriyama T, Ishii K, et al. Effects of IL-6 adiponectin, CRP and metabolic syndrome on subclinical atherosclerosis. Clin Chim Acta 2007;384:99–104.
[26] Cassidy AE, Bielak LF, Zhou Y, et al. Progression of subclinical coronary atherosclerosis: does obesity make a difference? Circulation 2005;111:1877–82.
[27] Hayashi T, Boyko EJ, McNeely MJ, et al. Minimum waist and visceral fat values for identifying the Japanese Americans at risk for metabolic syndrome. Diab Care 2007;30:120–7.
[28] Wong ND, Sciammarella MG, Polk D, et al. The metabolic syndrome, diabetes, and subclinical atherosclerosis assessed by coronary calcium. J Am Coll Cardiol 2003;41:1547–53.
[29] Hassinen M, Komulainen P, Lakka TA, et al. Metabolic syndrome and the progression of carotid intima-media thickness in elderly women. Arch Intern Med 2006;166:444–9.
[30] Horiguchi J, Yamamoto H, Akiyama Y, et al. Coronary artery calcium scoring using 16-MDCT and a retrospective ECG-gating reconstruction algorithm. Am J Roentgenol 2004;183:103–8.

Please cite this article in press as: Ohashi N, et al., Visceral fat accumulation as a predictor of coronary artery calcium as assessed by multislice computed tomography in Japanese patients, Atherosclerosis (2008), doi:10.1016/j.atherosclerosis.2008.04.019

Circulation J., in submission.

Noncalcified coronary plaque characteristics assessed by multislice computed tomography and serum lipid profiles as a function of different levels of statin therapy

Toshiro Kitagawa, MD, Hideya Yamamoto, MD, Jun Horiguchi, MD*,
Norihiko Ohhashi, MD, Eiji Kunita, MD, Hiroto Utsunomiya, MD, Yasuki Kihara, MD
Department of Cardiovascular Medicine, Graduate School of Biomedical Sciences, Hiroshima University, Hiroshima, Japan
*Department of Clinical Radiology, Hiroshima University Hospital, Hiroshima, Japan

Short title: Statin, lipid profile, and coronary plaque on MSCT

Address for correspondence: Hideya Yamamoto, MD, Department of Cardiovascular Medicine, Graduate School of Biomedical Sciences, Hiroshima University, 1-2-3 Kasumi Minami-ku, Hiroshima 734-8551, Japan.
Tel: +81-82-257-5540
Fax: +81-82-257-1569
E-mail: hideyayama@hiroshima-u.ac.jp

Total number of pages: 20
Total number of tables and figures: 6

Abstract

Background

We previously showed that densities within coronary plaques measured by multislice computed tomography (CT) reflect plaque components. We, therefore, evaluated whether characteristics of noncalcified coronary atherosclerotic lesions (NCALs) assessed by 64-slice CT angiography (CTA) were influenced by preceding

statin therapy and were related to serum lipid profiles.

Methods and Results

Of 150 patients with stable coronary artery disease who underwent CTA, 94 having 196 NCALs were studied retrospectively. Each NCAL was evaluated with the minimum CT density, and <40 Hounsfield units was considered lipid-rich. Among 3 groups classified by statin use continuing during >6-months preceding CTA (intensive [atorvastatin or rosuvastatin], n=23; moderate [pravastatin or simvastatin], n=23; none, n=48), the number of all NCALs per patient was similar (2.0±0.9 vs. 2.1±1.2 vs. 2.1±1.0), while that of lipid-rich NCALs per patient was lower in the intensive-statin group (0.5±0.6 vs. 1.2±0.9 vs. 1.1±0.9, p=0.008). Otherwise, among 3 groups with 0, 1, and ≥2 lipid-rich NCALs per patient, low-density lipoprotein cholesterol (LDL-C) / high-density lipoprotein cholesterol (HDL-C) ratios were substantially different (1.9±0.6, 2.1±0.9 and 2.9±1.1, p=0.0003).

Conclusions

Our study using CTA suggests that lower LDL-C/HDL-C is associated with fewer lipid-rich NCALs, and intensive statin therapy may change coronary plaques toward more stabilized.

Key words: Stain therapy; Lipid profile; Lipid-rich coronary plaque; Multislice computed tomography

Several lines of recent evidence suggest that lipid lowering therapy using

3-hydroxy-3-methylglutaryl coenzyme A reductase inhibitors (statins) reduce cardiovascular morbidity and mortality, and may even realize regression of coronary atherosclerosis.[1-3] Serial studies using intravascular ultrasound (IVUS) have demonstrated that regression of coronary atherosclerosis induced by intensive statin therapy is related to the greater reduction in low-density lipoprotein cholesterol (LDL-C) levels.[4-6] In addition, the benefits of intensive statin therapy may be also derived from increases in high-density lipoprotein cholesterol (HDL-C) levels.[7]

The latest technology of multislice computed tomography (MSCT) has the potential to identify and characterize non-calcified plaques in the coronary arteries in vivo.[9-10] We have reported that, in comparison with IVUS, 64-slice computed tomography (CT) enables equivalently reliable analyses of the components of non-calcified coronary atherosclerotic lesions (NCALs).[11] Densities within coronary plaques measured by MSCT may reflect plaque components, such as lipid accumulation, fibrous tissues and calcium, and lipid-rich plaques are likely to show lower densities on CT than fibrous-rich ones.[12]

In the present study, we evaluated whether characteristics of noncalcified coronary atherosclerotic lesions (NCALs) assessed by 64-slice CT angiography (CTA) were influenced by preceding statin therapy and were related to serum lipid profiles.

Methods

Study Patients

From December 2006 to March 2008, we enrolled 150 consecutive patients with clinically proven or suspected coronary artery disease (95 men and 55 women, average age = 65 ± 10 years). Each had a stable clinical presentation (no symptoms with equivocal or positive cardiac stress test, or atypical chest pain, or stable exertional chest pain), and each underwent CTA for follow-up or diagnosis of coronary artery disease. Exclusion criteria for CTA included cardiac arrhythmias (i.e., atrial fibrillation or frequent paroxysmal premature beats), contraindications for contrast medium, unstable hemodynamic conditions, and ongoing or previous acute coronary syndrome (ST-segment elevation myocardial infarction, or non-ST-segment elevation myocardial infarction and unstable angina by Braunwald's criteria[13]). Patients with previous percutaneous coronary intervention and/or coronary artery bypass grafting also were excluded. The study was approved by our hospital's ethical committee, and written

informed consent was obtained from all patients.

For each enrolled patient, we measured serum fasting triglycerides (TG), total cholesterol (TC), LDL-C [calculated with the Friedewald equation (TG <400 mg/dl) or directly measured], and HDL-C within 4 weeks before the CTA procedure, and calculated LDL-C/HDL-C ratio. We examined traditional coronary risk factors including hypertension (systolic/diastolic blood pressure ≥140/90 mmHg, and/or current use of antihypertensive agents), hyperlipidemia (TG ≥150mg/dl or TC ≥220 mg/dl or LDL-C ≥140 mg/dl, and/or current use of lipid-lowering agents), diabetes mellitus (glycohemoglobin A1c ≥6.5% and/or current use of hypoglycemic agents), and current smoking. In addition, we examined drug usage (intensive statins [IS; atorvastatin or rosuvastatin], moderate statins [MS; pravastatin or simvastatin], angiotensin-converting enzyme inhibitors [ACE-I] or angiotensin II receptor blockers [ARB], and aspirin) continuing during >6-months preceding the CTA. We enrolled no patients receiving statins other than listed above. We divided the patients into the 3 groups by their statin use (IS, MS, and no statin [NS] groups). We chose this medication period (>6-months) based on a report regarding the effect of statin therapy on coronary lesions in Japanese.[5]

MSCT scan protocol and reconstruction

Multislice computed tomographic angiography by an electrocardiographic gated method was performed using a 64-slice CT scanner (LightSpeed VCT, GE Healthcare, Waukesha, Wisconsin; gantry rotation time, 0.35 s; 64 x 0.625 mm detector collimation). Patients with a resting heart rate of ≥60 beats/min received 40 mg metoprolol orally 60 min before MSCT scanning; all received 0.3 mg nitroglycerin sublingually just before scanning. Our scan protocol and reconstruction method were described previously.[11, 14] In brief, after a plain scan to determine the calcium burden of the coronary tree and measure coronary calcium scores according to the standard Agatston method (sequential scan with 16 x 2.5 mm collimation; tube current, 140 mA; tube voltage, 120 kV), we performed contrast-enhanced scanning using 30 to 50 ml (0.6–0.7 ml/kg) contrast medium (Iopamidol, 370 mg I/ml, Bayer Healthcare, Berlin, Germany) during an inspiratory breath-hold. Volume data sets were acquired in the helical mode (64 x 0.625 mm collimation; CT pitch factor, 0.18–0.24:1; tube current, 600–750 mA with ECG-modulation technique; tube voltage, 120 kV). The effective radiation dose was estimated based on the dose-length product and ranged from 15 to 18 mSv.[11] Image reconstruction was performed using image-analysis software (CardIQ™, GE Healthcare) on a dedicated computer workstation (Advantage Workstation Ver.4.2,

GE Healthcare). A 'standard' kernel was used as the reconstruction filter. Either a half (temporal window = 175 milliseconds) or a multi-sector (temporal window <175 milliseconds) reconstruction algorithm was selected, and the optimal cardiac phase with the least motion artifacts was chosen individually.

Evaluation of NCAL characteristics

All coronary segments >2 mm in diameter were evaluated by 2 blinded and independent observers with curved multiplanar reconstruction images. The examined vessels were viewed in images reconstructed along the axis of the vessel of interest and in cross-sectional images perpendicular to the center line of the vessel. The definitions of NCALs and coronary calcium were as follows[11, 14]: *NCAL*, a low-density mass of > 1 mm^2 in size, located within the vessel wall and clearly distinguishable from the contrast-enhanced coronary lumen and the surrounding pericardial tissue; *coronary calcium*, a structure on the vessel wall with a CT density above that of the contrast-enhanced coronary lumen, or with a CT density of > 120 Hounsfield units (HU) assigned to the coronary artery wall in a plain image. For NCALs and calcium analyses, the optimal image display setting was chosen on an individual basis; in general, the window was between 700 and 1000 HU and the level between 100 and 200 HU.

As previously described, we evaluated NCAL characteristics on CTA.[11, 14] First, we decided NCAL size (small or large based on visual assessment with a threshold of 50% of vessel diameter), and assessed calcium deposits in or adjacent to each NCAL by determining its presence or absence and morphology as follows: diffuse, length (L) of calcium burden ≥ 3/2 of vessel diameter (VD) and width (W) ≥ 2/3 of VD; medium, L ≥ 3/2 of VD and W < 2/3 of VD or L < 3/2 of VD and W ≥ 2/3 of VD; spotty, L < 3/2 of VD and W < 2/3 of VD. Next, we determined the minimum CT density for each NCAL density by placing at least 5 regions of interest (area = 1 mm^2) in each lesion and documenting the lowest value of those, and, based on our previous results[11], low-density NCALs were defined as lesions with a minimum CT density of <40 HU. We considered low-density NCALs as lipid-rich, while we excluded any lesion with a CT density >120 HU from NCALs because of the high probability of a calcified plaque.[8] Then, we measured the CT density of a region of interest (area = 1 mm^2) positioned in the center of each reference site lumen as the contrast density within the coronary lumen. When the definition of NCAL and the classification of NCAL size and adjacent calcium deposits varied among the observers, the determination was achieved by consensus of

the observers.

Statistical analysis

Coronary calcium score is expressed as median value and range, and other measurements are expressed as mean ± SD. The Mann-Whitney test and analysis of variance (ANOVA) were performed to compare continuous variables between the 2 groups and among the 3 or 4 groups, respectively. Categorical variables were compared using the chi-square test. Linear regression was used to examine factors related to the number of lipid-rich NCALs per patient for multivariate analysis. Interobserver variability of measured CT densities was determined by calculating Pearson's correlation coefficient. All analyses were performed using JMP 5.0.1 statistical software (SAS Institute Inc, North Carolina). A P value of < 0.05 was considered statistically significant.

Results

During contrast-enhanced CT scanning, mean heart rate was 63 ± 8 beats/min, and mean scan time was 6.4 ± 1.9 s. No patient experienced any complication due to the CT scanning, and no patient was excluded from analysis due to poor image quality of the CTA.

Of the 150 patients, 56 (36%) had no NCALs (no coronary atherosclerotic lesions, or only calcified coronary lesions) as detected by CTA. In the remaining 94 patients (64%), a total of 196 NCALs (n = 2.1 ± 1.0, range, 1–5 lesions per patient) were detected. **Table 1** shows clinical characteristics, drug usage, coronary calcium scores, and serum lipid profiles of the 94 patients with NCALs. Patients were divided into 3 groups according to their statin use (IS, n = 23; MS, n = 23; NS, n = 48). The doses of each statin were 10–20 mg/day of atorvastatin, 2.5–10 mg/day of rosuvastatin, 10–20 mg/day of pravastatin, and 5–10 mg/day of simvastatin, respectively. There were no significant differences in the clinical characteristics among the 3 groups, except for hyperlipidemia. ACE-I or ARB were used more by the IS group, and aspirin by the MS group. Serum TC, LDL-C levels, and LDL-C/HDL-C ratio were lower in the IS group than the others.

Table 2 shows the comparison of NCAL distribution and morphological findings among the 3 groups classified by statin use (IS, 47 lesions; MS, 48 lesions; NS, 101

lesions). The location, size, proportion of obstructive lesions (≥ 75% stenosis on CTA), and adjacent calcium morphology of NCALs were similar among the 3 groups. Excellent interobserver agreement was found for minimum CT densities of NCALs (r = 0.89), and for CT densities of reference site lumens (r = 0.92). Of all 196 NCALs, 94 lesions (48%, n = 1.0 ± 0.9, range, 0–4 lesions per patient) were defined as lipid-rich. The minimum CT density of NCALs in the IS group was significantly higher than in the other 2 groups (53 ± 22 vs. 41 ± 30 vs. 40 ± 28 HU, p = 0.02) (**Fig 1**). There was no difference in mean CT densities of reference site lumens among the 3 groups (349 ± 41 vs. 363 ± 49 vs. 348 ± 63 HU, p = 0.28). **Table 3** shows the comparison of NCAL detection by CTA among the 3 groups. The number of all NCALs per patient was similar among the 3 groups, while that of lipid-rich NCALs per patient was lower in the IS group than in the others. In addition, there were more patients with absence of lipid-rich NCALs in the IS group.

Table 4 shows the comparisons of serum lipid profiles among the 3 groups classified by the number of lipid-rich NCALs per patient (absence, n = 27; 1 lesion, n = 47; ≥2 lesions, n = 20). LDL-C, HDL-C levels, and LDL-C/HDL-C ratio were significantly different among the 3 groups. LDL-C/HDL-C ratios were substantially higher in patients with ≥2 lipid-rich NCALs than in those with no or 1 lesion, and the difference in LDL-C/HDL-C ratios among the 3 groups was the most significant. **Fig 2** shows representative MSCT findings in a case having no lipid-rich NCALs under intensive statin therapy, and in a case having multiple lipid-rich NCALs under moderate statin therapy.

On multivariate analysis (adjusted for age, gender, coronary risk factors, drug uses, and LDL-C/HDL-C ratio), intensive statin use was independently related to a decreased number of lipid-rich NCALs per patient (regression coefficient -0.33, 95% CI -0.63 to -0.02, p = 0.04), while LDL-C/HDL-C ratio was independently related to an increased number of lipid-rich NCALs per patient (regression coefficient 0.21, 95% CI 0.01 to 0.42, p = 0.04).

Discussion

In the present study, we demonstrated that patients with stable coronary artery disease undergoing intensive statin therapy for >6-months have fewer lipid-rich NCALs on CTA using 64-slice CT than do patients undergoing moderate or no statin therapy. In

addition, to the best of our knowledge, the present study is the first to report that a high LDL-C/HDL-C ratio is most strongly related to multiple (≥2) lipid-rich NCALs on CTA. Multivariate analysis revealed that intensive statin use independently determines fewer lipid-rich NCALs on CTA, and that, inversely, a higher LDL-C/HDL-C ratio independently determines more lipid-rich NCALs on CTA. Our findings support the concept that intensive statin therapy stabilizes coronary plaques, and suggest the close relationship between LDL-C/HDL-C ratio and coronary plaque characteristics.

Computed tomography density for coronary plaque characteristics

It has been reported that CT densities measured within coronary plaques reflect the plaque components predicted by the echogenity on IVUS.[15] In most MSCT of various studies, coronary plaque densities have been defined by averaging some density measurements. However, these methods are assumed to be more susceptible to various artifacts and interobserver variability. These methods, therefore, may contribute to a substantial overlap of CT density between fibrous and soft plaques.[15] Our method of selecting the single and minimum density value as NCAL density has been approved to be a method for limiting the influence of partial volume and beam hardening effects resulting from neighboring structures, especially hyperdense calcium, and for minimizing interobserver variability for plaque CT density determination. [11, 14] In a prospective study using MSCT coronary angiography, patients with low-density coronary plaques defined by the minimum CT density were more likely to have acute coronary syndromes than patients without low-density coronary plaques.[16] Therefore, the minimum CT density that we applied in this study is applicable as an indicator of NCAL characteristics related to future coronary events.

Effect of intensive statin on coronary plaque characteristics

In the present study, lipid-rich NCALs on CTA are less frequently observed in patients under intensive statin therapy. Of particular note is the fact that intensive statin use remains an independent predictor of fewer lipid-rich coronary plaques on the multivariate analysis after adjusting for LDL-C/HDL-C ratio. Although the number of patients undergoing intensive statin therapy was relatively small, these findings may indicate a direct effect of intensive statin on coronary plaque characteristics, and may suggest that the regression of coronary plaque volume by intensive statin therapy on

IVUS[4-7] results from a reduction in the lipid component, subsequently leading to fewer lipid-rich coronary plaques.

Relationship between coronary plaque characteristics and LDL-C/HDL-C ratio

In the present study, higher LDL-C is related to multiple lipid-rich NCALs. This finding indicates that excessive serum LDL-C contributes to coronary atheroma expansion through the modification to an oxidized form and ingestion by macrophages via scavenger receptors.[17] Therefore, maintaining a lower LDL-C level by statin therapy is beneficial for the prevention of lipid-rich NCAL initiation and progression. More importantly, the present study demonstrates the close relationship between higher LDL-C/HDL-C ratio and multiple lipid-rich NCALs. Recent reports demonstrated that infusing reconstituted HDL-C particles containing apoA-1 Milano promoted regression of coronary atherosclerosis in humans following acute coronary syndrome,[18] and that intravenous infusion of a single dose of reconstituted HDL led to acute changes in plaque characteristics with a reduction in lipid content.[19] These reports indicate that raising HDL-C which has a central role in reverse transmission of serum cholesterol causes regression of coronary atherosclerosis with a reduction in lipid content. In line with these reports and the previous IVUS data,[7] our findings also indicate the importance not only of reductions in LDL-C levels, but also, of increases in HDL-C levels by statin therapy for regressing coronary plaque volume and subsequently decreasing lipid-rich coronary plaques.

Study limitations

The present study is limited by the lack of measurement of C-reactive protein, because the relationship between lipids, inflammation, and their effect on the arterial wall has been of considerable interest. In addition, the present study includes several limitations in interpretation of CT densities of NCALs. First, a low-density NCAL is indistinguishable from thrombosis due to their similar densities, and we cannot completely exclude the possibility that thrombosis may be present in some coronary lesions. However, this study included only patients with stable coronary artery disease, who might not have newly-developed thromboses in their coronary arteries. Second,

contrast density within the coronary lumen and severe calcium deposits may have an influence on the density values measured within coronary plaques. In the present study, there was no significant difference in coronary lumen density and adjacent calcium morphology of NCALs between the respective groups. However, a method having smaller differences in coronary lumen density among the lesions is required to compare the coronary plaque densities more precisely. Although our selecting the minimum density value as NCAL density is expected to be less susceptible to artifacts from the coronary lumen and calcium deposits, it remains difficult to determine the definite composition of individual NCALs with current CT resolution. Finally, this study was designed as a retrospective study, and prospective studies in a large population are required to confirm the benefits of statin therapy and LDL-C/HDL-C ratio lowering on coronary plaque stabilization.

Conclusions

Our CTA findings support the concept that intensive statin therapy stabilizes coronary plaques, and indicate the close relationship between LDL-C/HDL-C ratio and coronary plaque characteristics. Further prospective studies are needed to monitor coronary plaque stabilization in patients under intensive stain therapy using CTA, with reference to the level of LDL-C/HDL-C ratio.

Acknowledgements

We are grateful to Noriaki Matsuura, MD, Masao Kiguchi, RT, and Chikako Fujioka, RT, for their technical assistance. We also thank Dr. Shozo Miki for his critical reading of the manuscript.

References

1. Downs JR, Clearfield M, Weis S, Whitney E, Shapiro DR, Beere PA, et al. Primary prevention of acute coronary events with lovastatin in men and women with average cholesterol levels: results of AFCAPS/TexCAPS. (Air Force/Texas Coronary Atherosclerosis Prevention Study.) *JAMA* 1998; **279**: 1615-1622.

2. Yokoi H, Nobuyoshi M, Mitsudo K, Kawaguchi A, Yamamoto A. Three-year follow-up results of angiographic intervention trial using an HMG-CoA reductase inhibitor to evaluate retardation of obstructive multiple atheroma (ATHEROMA) study. *Circ J* 2005; **69**: 875-883.

3. Itakura H, Kita T, Mabuchi M, Matsuzaki M, Matsuzawa Y, Nakaya N, et al. Relationship between coronary events and serum cholesterol during 10 years of low-Dose simvastatin therapy. *Circ J* 2008; **72**: 1218-1224.

4. Nissen SE, Nicholls SJ, Sipahi I, Libby P, Raichlen JS, Ballantyne CM, et al. Effect of very high-intensity statin therapy on regression of coronary atherosclerosis: the ASTEROID trial. *JAMA* 2006; **295**: 1556-1565.

5. Okazaki S, Yokoyama T, Miyauchi K, Shimada K, Kurata T, Sato H, et al. Early statin treatment in patients with acute coronary syndrome: demonstration of the beneficial effect on atherosclerotic lesions by serial volumetric intravascular ultrasound analysis during half a year after coronary event: the ESTABLISH Study. *Circulation* 2004; **110**: 1061-68.

6. Takashima H, Ozaki Y, Yasukawa T, Waseda K, Asai K, Wakita Y, et al. Impact of lipid-lowering therapy with pitavastatin, a new HMG-CoA reductase inhibitor, on regression of coronary atherosclerotic plaque. *Circ J* 2007; **71**: 1678-84.

7. Nicholls SJ, Tuzcu EM, Sipahi I, Grasso AW, Schoenhagen P, Hu T, et al. Statins, high-density lipoprotein cholesterol, and regression of coronary atherosclerosis. *JAMA* 2007; **297**: 499-508.

8. Schroeder S, Kopp AF, Baumbach A, Meisner C, Kuettner A, Georg C, et al.

Noninvasive detection and evaluation of atherosclerotic coronary plaques with multislice computed tomography. *J Am Coll Cardiol* 2001; **37**: 1430-1435.

9. Hausleiter J, Meyer T, Hadamitzky M, Kastrati A, Martinoff S, Schömig A. Prevalence of noncalcified coronary plaques by 64-slice computed tomography in patients with an intermediate risk for significant coronary artery disease. *J Am Coll Cardiol* 2006; **46**: 312-318.

10. Motoyama S, Kondo T, Anno H, Sugiura A, Ito Y, Mori K, et al. Atherosclerotic plaque characterization by 0.5-mm-slice multislice computed tomographic imaging. *Circ J* 2007; **71**: 363-366.

11. Kitagawa T, Yamamoto H, Ohhashi N, Okimoto T, Horiguchi J, Hirai N, et al. Comprehensive evaluation of non-calcified coronary plaque characteristics detected using 64-slice computed tomography in patients with proven or suspected coronary artery disease. *Am Heart J* 2007; **154**: 1191-1198.

12. Nikolaou K, Becker CR, Muders M, Babaryka G, Scheidler J, Flohr T, et al. Multidetector-row computed tomography and magnetic resonance imaging of atherosclerotic lesions in human ex vivo coronary arteries. *Atherosclerosis* 2004; **174**: 243-52.

13. Braunwald E, Antman EM, Beasley JW, Califf RM, Cheitlin MD, Hochman JS, et al. ACC/AHA 2002 guideline update for the management of patients with unstable angina and non-ST-segment elevation myocardial infarction-summary article: a report of the American College of Cardiology/American Heart Association Task Force on Practice Guidelines (Committee on the Management of Patients With Unstable Angina). *J Am Coll Cardiol* 2002; **40**: 1366-1374.

14. Kitagawa T, Yamamoto H, Horiguchi J, Ohhashi N, Tadehara F, Shokawa T, et al. Characterization of noncalcified coronary plaques and identification of culprit lesions in patients with acute coronary syndrome by 64-slice computed tomography. *J Am Coll Cardiol Img* 2009; **2**: 153-60.

15. Leber A, Knez A, Becker A, Becker C, von Ziegler F, Nikolaou K, et al. Accuracy

of multidetector spiral computed tomography in identifying and differentiating the composition of coronary atherosclerotic plaques: a comparative study with intracoronary ultrasound. *J Am Coll Cardiol* 2004; **43**: 1241-1247.

16. Matsumoto N, Sato Y, Yoda S, Nakano Y, Kunimasa T, Matsuo S, et al. Prognositic value of non-obstructive CT low-dense coronary artery plaques detected by multislice computed tomography. *Circ J* 2007; **71**: 1898-1903.
17. Hansson GK. Inflammation, atherosclerosis, and coronary artery disease. *N Eng J Med* 2005; **352**: 1685-1695.
18. Nissen SE, Tsunoda T, Tuzcu EM, Schoenhagen P, Cooper CJ, Yasin M, et al. Effect of recombinant Apo-A-1 Milano on coronary atherosclerosis in patients with acute coronary syndromes: a randomized controlled trial. *JAMA* 2003; **290**: 2292-2300.
19. Shaw JA, Bobik A, Murphy A, Kanellakis P, Blombery P, Mukhamedova N, et al. Infusion of reconstituted high-density lipoprotein leads to acute change in human atherosclerotic plaque. *Circ Res* 2008; **103**: 1084-1091.

Figure legends

Fig 1. Comparison of minimum CT densities of all NCALs among the 3 groups

classified by statin use (intensive [n = 47], moderate [n = 48], and no statin [n = 101] groups) (53 ± 22 vs. 41 ± 30 vs. 40 ± 28 HU, p = 0.02).

Fig 2. Case 1. A case of 75 year-old male receiving atorvastatin (10 mg/day). Serum low-density lipoprotein cholesterol (LDL-C), high-density lipoprotein cholesterol (HDL-C), and LDL-C/HDL-C ratio were 81mg/dl, 45 mg/dl, and 1.8, respectively. Curved multiplanar reconstruction (MPR) images show NCALs in the right coronary artery (RCA) (arrowheads; a, b), and the minimum CT densities of those were 46 and 63 HU, respectively. Case 2. A case of 74 year-old male receiving pravastatin (10 mg/day). Serum LDL-C, HDL-C, and LDL-C/HDL-C ratio were 183mg/dl, 45mg/dl, and 4.1, respectively. Curved MPR images show NCALs in RCA (arrowheads; c, d), and the minimum CT densities of those were 34 and 16 HU, respectively.

Figure 1

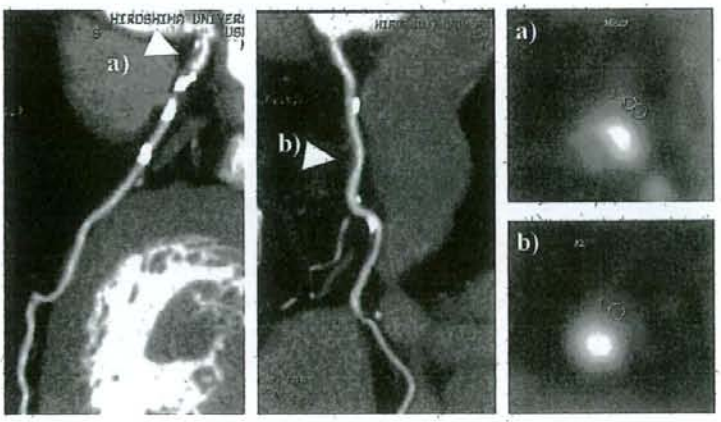

Figure 2

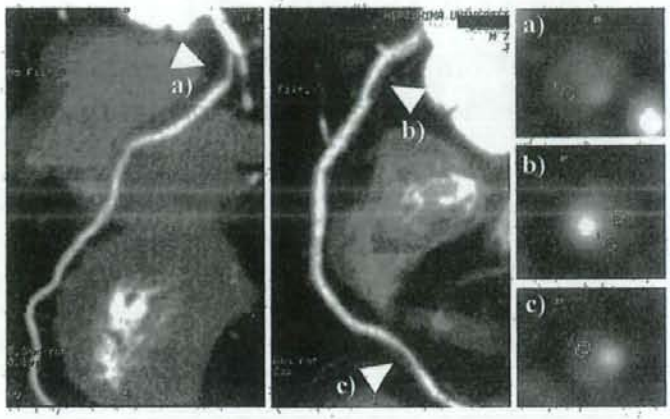

Circ J 2009; **73:** 691–698

Diagnostic Accuracy of Angiographic View Image for the Detection of Coronary Artery Stenoses by 64-Detector Row CT

— A Pilot Study Comparison With Conventional Post-Processing Methods and Axial Images Alone —

Masahiro Jinzaki, MD; Kozo Sato, MD; Yutaka Tanami, MD; Minoru Yamada, MS*; Toshihisa Anzai, MD**; Akio Kawamura, MD**; Koji Ueno, MD**; Sachio Kuribayashi, MD

Background: The angiographic view (AGV) image is a new post-processing method that is similar to conventional coronary angiography (CAG). The purpose of this study was to evaluate its accuracy for coronary stenosis detection by 64-detector row computed tomography (CT).

Methods and Results: CT evaluation results of 17 patients were compared with the results of invasive CAG on a coronary segment basis concerning the presence of stenoses >50% diameter reduction. All images of the 3 viewing methods (combination of conventional methods, AGV image alone, and axial images alone) were evaluated in consensus by 3 cardiovascular radiologists. Among 196 assessable segments, invasive CAG showed significant coronary artery stenoses in 44 segments. 43 of 44 lesions were detected with the AGV image, and absence of significant stenosis was correctly identified in 135 of 152 segments (sensitivity 98%; specificity 89%; accuracy 91%; positive predictive value 72%, negative predictive value 99%). The sensitivity of the AGV image was the same as that of conventional methods (98%). There was no significant difference in accuracy between the AGV image (91%) and conventional methods (94%). The accuracy of the AGV image was significantly higher than the axial images alone (78%).

Conclusions: AGV image shows promise as a post-processing method for identifying coronary artery stenosis with high accuracy. (*Circ J* 2009; **73:** 691–698)

Key Words: Computed tomography; Coronary angiography; Coronary artery disease; Maximum-intensity projection; Post-processing

Recent advances in multidetector-row computed tomography (MDCT) have enabled non-invasive evaluation of coronary artery stenoses with high accuracy!–4 Diagnostic evaluation of coronary artery stenoses includes review of the originally reconstructed axial images, as well as various post-processing images. The important role of post-processing images is to integrate the series of axial CT sections into a form that is easier to interpret and the axial images can be made to appear similar to other, more familiar images such as those from invasive angiography?–9 In these aspects, current methods, such as volume rendering (VR), partial maximum intensity projection (partial MIP), curved multiplanar reconstruction (curved MPR), or cross-sectional images, fall short. VR enables overview of the coronary artery to third parties, but it is not usually used for the evaluation of coronary artery stenoses. For coronary artery stenoses, partial MIP, curved MPR or cross-sectional images are used, but these conventional methods are quite different from the images obtained with invasive coronary angiography (CAG), and it can be difficult for a third person to understand which artery or segment is being analyzed.

The angiographic view (AGV) image is a MIP image in which contrast media in the ventricles is eliminated? This image is similar to that from invasive CAG and thus familiar to cardiologists. This type of MIP image clearly demonstrates the distribution of high-density lesions, such as coronary calcifications and stents, in the 1 image. If coronary artery stenoses can also be identified on the AGV image with high accuracy, it will be the post-processing method with most promise for accurately showing the distribution of coronary lesions that is understandable by third parties such as referral physicians and the patients.

In this study, we evaluated the accuracy of the AGV image in comparison with axial images alone and a combination of conventional methods for coronary stenoses detection.

(Received August 18, 2008; revised manuscript received November 21, 2008; accepted December 7, 2008; released online February 18, 2009)
*Department of Diagnostic Radiology, *Division of Cardiovascular Imaging Laboratory, Research Park and **Division of Cardiology, Department of Medicine, Keio University School of Medicine, Tokyo, Japan*

Mailing address: Masahiro Jinzaki, MD, Department of Diagnostic Radiology, Keio University School of Medicine, 35 Shinanomachi, Shinjuku-ku, Tokyo 160-8582, Japan. E-mail: jinzaki@sc.itc.keio.ac.jp

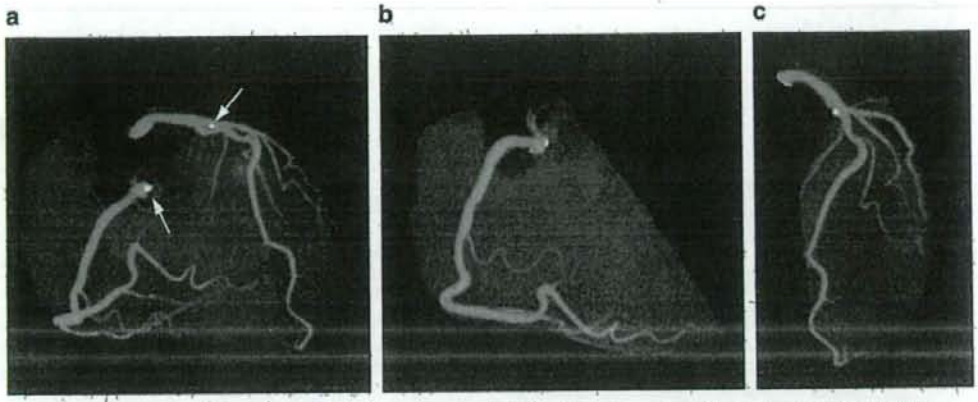

Figure 1. Angiographic view (AGV) of the coronary arteries (a) enables an overview of the coronary tree. The AGV is divided into right (b) and left (c) coronary artery, and viewed from various angles. The distribution of calcifications (arrows) is shown.

Table 1. Diagnostic Accuracy of Each Viewing Method: Test Characteristics by Segments

	Sensitivity	Specificity	PPV n/total n (%)	NPV	Accuracy
Angiographic view image	43/44 (98)	135/152 (89)	43/60 (72)	135/136 (99)	178/196 (91)
Conventional methods	43/44 (98)	141/152 (93)	43/54 (80)	141/142 (99)	184/196 (94)
Axial images alone	38/44 (86)	115/152 (76)	38/75 (51)	115/121 (95)	153/196 (78*)

*P<0.05 for angiographic view vs axial images alone and conventional methods vs axial images alone.
PPV, positive predictive value; NPV, negative predictive value.

Methods

Patient databases from the Catheter Angiography Laboratory and Radiology Department were reviewed for patients who had undergone both invasive CAG and CT CAG within 1 month and without other interventions in the meantime. We identified 18 consecutive patients from May 2005 to September 2005, but 1 was excluded because of atrial fibrillation. Thus, data of 17 patients (15 men, 2 women; 35–80 years, average 58 years) were available. The average heart rate (HR) of these patients was 58.6±6.6 beats/min (44–72 beats/min; 16 patients with HR<70 beats/min, 1 patient with HR>70 beats/min). Retrospective evaluation of patient data acquired during clinical routines is approved by the Institutional Review Board, and written informed consent was not obtained from the patients.

MDCT Data Acquisition

Computed tomography (CT) CAG was performed using 64-detector row CT (LightSpeed VCT; GE Healthcare, Milwaukee, WI, USA). Nitroglycerin spray (0.3 mg, glycerol trinitrate) was administered sublingually immediately before the scan; β-blocker was not administered prior to the scan. The delay between the start of injection and scanning was determined by the test bolus technique, monitoring at the level of the ascending aorta. The dynamic monitoring scans started 10 s after beginning the injection of intravenous contrast material (10 ml of contrast material followed by 15 ml of saline injected at 4 ml/s), and were obtained every 2 s with low-dose (120 kV, 20 mA). The delay applied for the main scanning was calculated by the time to peak enhancement for the test bolus plus 2 s. The main scanning was performed with 64×0.625 mm collimation, acquiring the entire heart within 5 to 6 s. The gantry rotation time was 0.35 s, and the pitch was between 0.20 and 0.22. The tube current was 350–550 mA at 120 kV. Iodine contrast material (40–60 ml; Iopamidol 370 mgI/ml) was immediately followed by 20 ml of saline, injected at a rate of 4 ml/s. The estimated effective radiation dose was 15–19 mSv. ECG-gated datasets were reconstructed automatically at 75% of the R-R interval and 45% of the R-R interval to create a stack of contiguous axial images with a section thickness of 0.625 mm and an increment of 0.625 mm. Depending on the HR, 2 reconstruction algorithms were applied: a single-segmental reconstruction (<70 beats/min) and multisector (2 or 4) reconstruction (>70 beats/min). If motion artifacts were present in any coronary artery, image reconstruction was repeated with the reconstruction window offset by 5% toward the beginning or end of the cardiac cycle, and multiple reconstructions were obtained until all arteries were depicted free of motion artifact or until reconstructions in 5% intervals throughout the cardiac cycle had been obtained.

Invasive CAG

Invasive CAG was performed by experienced cardiologists using standard techniques and the acquisition of standard projection planes. Stenosis severity was determined by quantitative CAG (QCA) (QuantCor.QCA, Pie Medical Imaging, Maastricht, The Netherlands). The grade of diameter stenosis (maximum diameter reduction) was determined by dividing the minimal diameter in the diseased segment by the diameter in the adjacent proximal disease-free section.

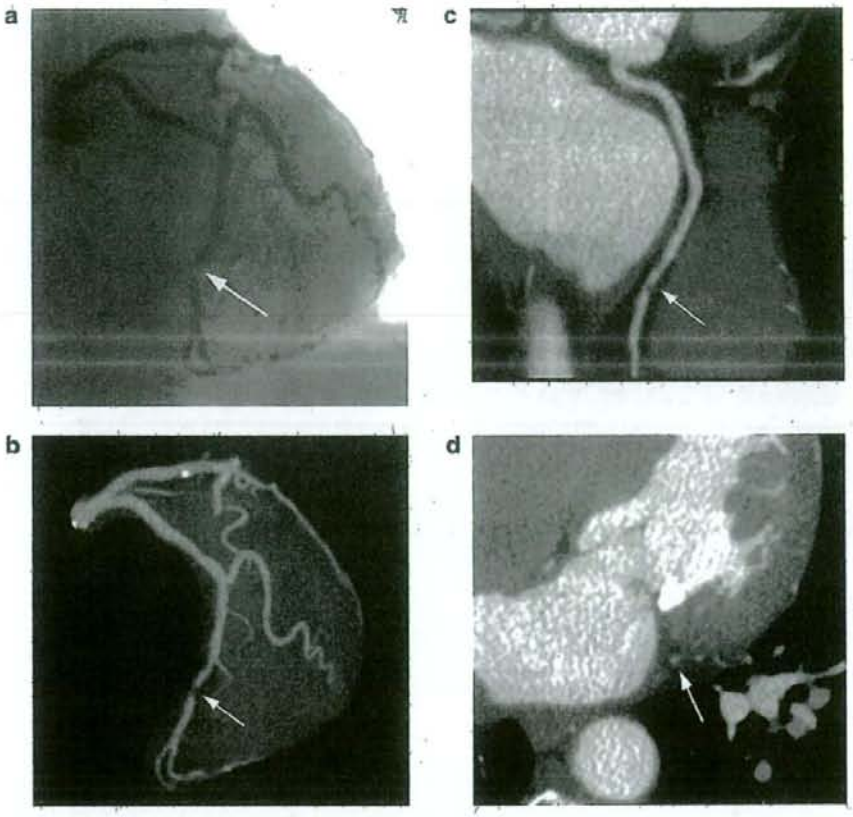

Figure 2. A 67-year-old woman with a significant stenosis in the distal left circumflex artery on the invasive angiogram (**a**: arrow). This lesion was correctly diagnosed as >50% stenoses with all viewing methods: angiographic view image (**b**: arrow), conventional methods (**c**: arrow), and axial images (**d**: arrow).

MDCT Image Analysis

CT axial images were transferred to a standard commercial workstation (GE Advantage Workstation 4.3) where the AGV image was automatically created as follows.

(1) The whole heart is extracted from the 3D volume data, after cutting and removing unnecessary regions such as bone, aorta and liver.

(2) Contrast medium within the endocardium is identified as ventricular.

(3) The ventricular area is subtracted from the whole heart image.

(4) MIP display of the image shows the coronary artery network identical to that seen with invasive CAG.

The AGV image can be spun around and viewed in various angles. Similar images can be created by tracking and extracting the coronary artery itself. However, tracking or extracting requires the threshold of CT attenuation, so the images can vary depending on the threshold, and the ability of the workstation used. The AGV image keeps the coronary artery untouched, and thus the image does not vary among workstations.

One technologist (4 years experience in cardiac CT imaging) who was unaware of the results of conventional CAG rendered curved MPR and AGV images. Curved MPRs were rendered with 0.6-mm section thickness, displaying all 15 segments of the AHA model in 2 orientations (with longitudinal and cross-sectional images as reference). Whether each coronary segment seen on the axial images was also identified by the conventional methods and on the AGV image was checked by this blinded technologist. The data sets were then stored for further analysis.

All images for the 3 viewing methods (ie, combination of conventional methods [axial images, partial MIP, partial MPR, and curved MPR], AGV image alone, and axial images alone) were evaluated in consensus by 3 cardiovascular radiologists: 2 with 5 years experience and 1 with 4 years experience in CT CAG. The readers were unaware of the patient's history, clinical details and QCA findings. First, the conventional methods were assessed, then the AGV image alone, and lastly the axial images alone, all at 2-week intervals. In the reading of the conventional methods, the readers interactively rendered partial MPRs or partial MIPs by using a 0.6-mm-thickness, and comprehensively reviewed these images, the axial images, and curved MPRs on the workstation. Axial images and curved MPRs were initially displayed with a default window setting (level, 100 HU; window, 700 HU). The AGV image was divided into the right and left coronary artery, similar to images from invasive CAG, and the readers viewed various angles of the images (**Figure 1**). The AGV image was initially dis-

Table 2. Location of False-Negative Lesions of Each Viewing Method

	Vessel branching out from mid-portion of the stent	Lesion located in the just proximal portion of the branch	Lesion located at the segment running horizontal to the axial section	Total
Angiographic view image	1	0	0	1
Conventional methods	0	1	0	1
Axial images alone	1	0	5	6

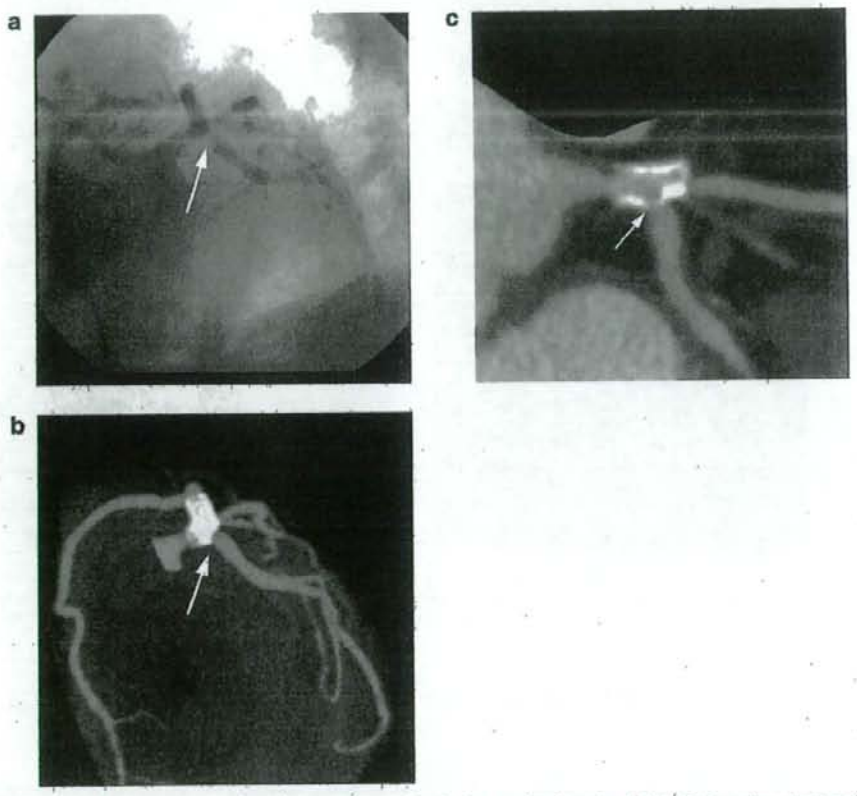

Figure 3. A 55-year-old man with a significant stenosis in the just proximal portion of the left circumflex artery on the invasive angiogram (**a**: arrow). This lesion was not detected (false negative) on the angiographic view image (**b**: arrow), but was correctly diagnosed as >50% stenosis by the conventional methods (**c**: arrow) and on the axial images (not shown).

played with a default window setting (level, 350 HU; window, 700 HU). The window and level of the evaluated images was then adjusted by the observer. Segments with severe calcifications (occupying more than half the circumference), stents, a vessel caliber less than 1.5 mm as defined on conventional CAG, or with a discontinuous area because of premature beat were excluded from the analysis.

All analyses were performed on a coronary segment basis (15 segments of the AHA model). Each segment was categorized by the presence or absence of a stenoses of 50% diameter reduction or more. MDCT evaluation results were documented in writing and then compared with the results of QCA. True positives were defined as correct identification by MDCT of segments of more than 50% diameter and true negatives were defined as correct identification by MDCT of segments of 50% or less. Segments that had inconsistencies between QCA and each viewing method were retrospectively re-evaluated by the 3 radiologists.

Statistical Analysis

The sensitivity, specificity, positive predictive value (PPV), and negative predictive value (NPV) of each of the viewing methods for detection of hemodynamically significant stenoses (≥50%) as compared with the reference standard (QCA) were calculated for each segment. We compared the accuracy of the different viewing methods for the detection of stenoses using McNemar's test. Statistical significance was considered to be present at $P<0.05$. Statistical analysis was performed using SPSS (version 13.0; SPSS, Chicago, IL, USA).